

## Supporting Information

# Tetrakis (4-carboxyphenyl) porphyrin and $\text{Ru}(\text{bpy})_3^{2+}$ modified $\text{SiO}_2$ nanosphere for potential and wavelength resolved electrochemiluminescence

Mingquan Guo, Jiangnan Shu\*, Dexin Du, Yisha Wang, Hua Cui\*

Key Laboratory of Precision and Intelligent Chemistry, iChEM (Collaborative Innovation Center of Chemistry for Energy Materials), Department of Chemistry, University of Science and Technology of China, Hefei, Anhui 230026, P. R. China.

### Corresponding Author

**Hua Cui**

Fax: +86-551-63600730.

\*E-mail: [hcui@ustc.edu.cn](mailto:hcui@ustc.edu.cn).

**Jiangnan Shu**

\*E-mail: [jiangnan@ustc.edu.cn](mailto:jiangnan@ustc.edu.cn).

### S1. Preparation of CRuSiO<sub>2</sub> NPs

CRuSiO<sub>2</sub> NPs were synthesized through the W/O microemulsion system<sup>1</sup>. The W/O microemulsion system was prepared first by mixing 1.77 mL of TX-100, 7.5 mL of cyclohexane, 1.8 mL of 1-hexanol, and 100  $\mu$ L 0.5% chitosan. Then 400  $\mu$ L 2.5 mM Ru(bpy)<sub>3</sub><sup>2+</sup> aqueous solution was added into the mixture. In the presence of 90  $\mu$ L of TEOS, a polymerization reaction was initiated by adding 60  $\mu$ L of NH<sub>3</sub>·H<sub>2</sub>O (25%–28%). The hydrolysis reaction was allowed to continue for 24 h. Acetone was then added to destroy the emulsion, followed by centrifuging and washing with ethanol and water. At last, the orange CRuSiO<sub>2</sub> NPs were obtained.

### S2. XPS Ru spectra of TCPP@CRuSiO<sub>2</sub> NPs

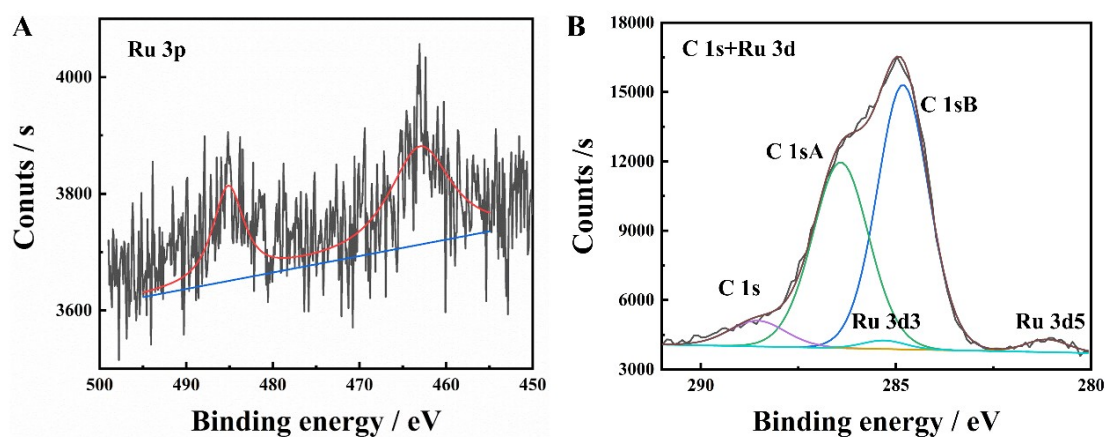


Figure S1. (A) Ru 3p spectra (B) C 1s and Ru 3d spectra of XPS of TCPP@CRuSiO<sub>2</sub>.

### S3. XRD patterns

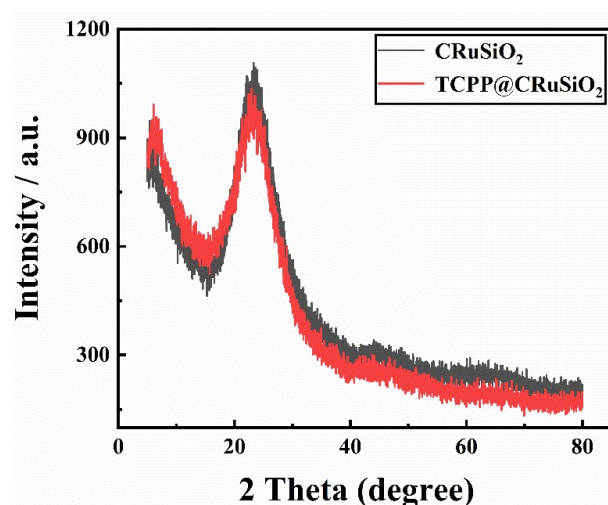
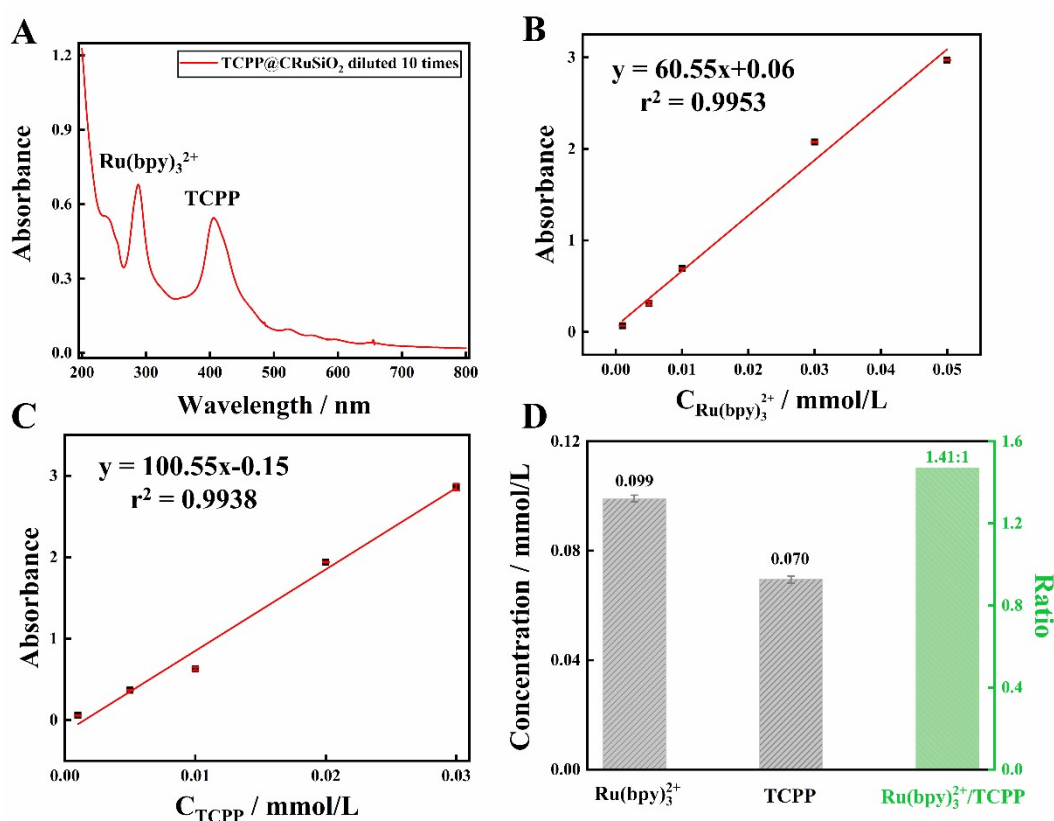


Figure S2. XRD patterns of CRuSiO<sub>2</sub> (black line) and TCPP@CRuSiO<sub>2</sub> (red line).

#### S4. Measurement of TCPP and Ru(bpy)<sub>3</sub><sup>2+</sup> content

As shown in Figure S3A, the UV-vis spectrum of TCPP@CRuSiO<sub>2</sub> showed two characteristic absorption peaks at 288 and 405 nm, which were attributed to Ru(bpy)<sub>3</sub><sup>2+</sup> and TCPP, respectively. Based on this, the concentrations of Ru(bpy)<sub>3</sub><sup>2+</sup> and TCPP were determined by the UV-vis spectrophotometry. First, the standard curves between the concentration and absorbance intensity of Ru(bpy)<sub>3</sub><sup>2+</sup> and TCPP were established as shown in Figure S3B and S3C, respectively. Then, the molar concentrations of TCPP and Ru(bpy)<sub>3</sub><sup>2+</sup> in TCPP@CRuSiO<sub>2</sub> were calculated to be 0.070 and 0.099 mmol/L, respectively. Thus, the molar ratio of TCPP to Ru(bpy)<sub>3</sub><sup>2+</sup> in TCPP@CRuSiO<sub>2</sub> was 1:1.41 (Figure S3D).



**Figure S3.** (A) UV-vis spectrum of TCPP@CRuSiO<sub>2</sub> diluted 10 times. Absorbance-concentration fitted curve of (B) Ru(bpy)<sub>3</sub><sup>2+</sup> and (C) TCPP. (D) Concentrations and molar ratio of Ru(bpy)<sub>3</sub><sup>2+</sup> and TCPP.

#### S5. SEM of TCPP@CRuSiO<sub>2</sub> modified GCE electrode

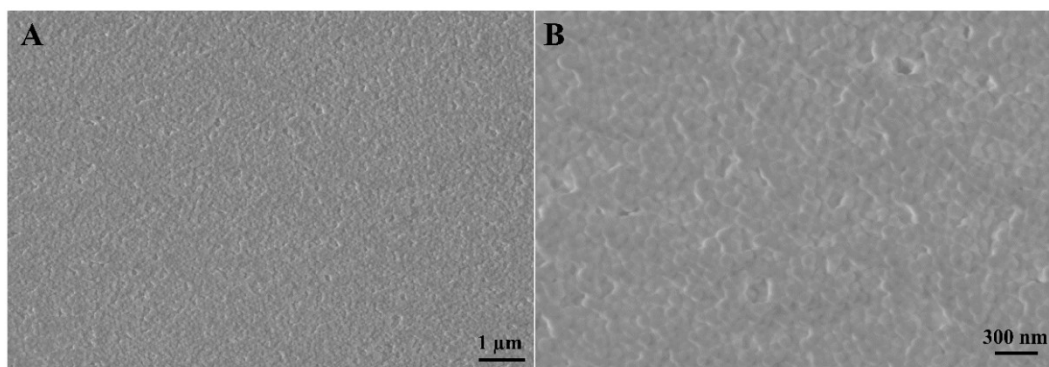


**Figure S4.** SEM images of TCPP@CRuSiO<sub>2</sub> modified GCE electrode in different scales: (A) 1 μm and (B) 300 nm.

### S6. Stacked spectra of ECL-1 and ECL-2

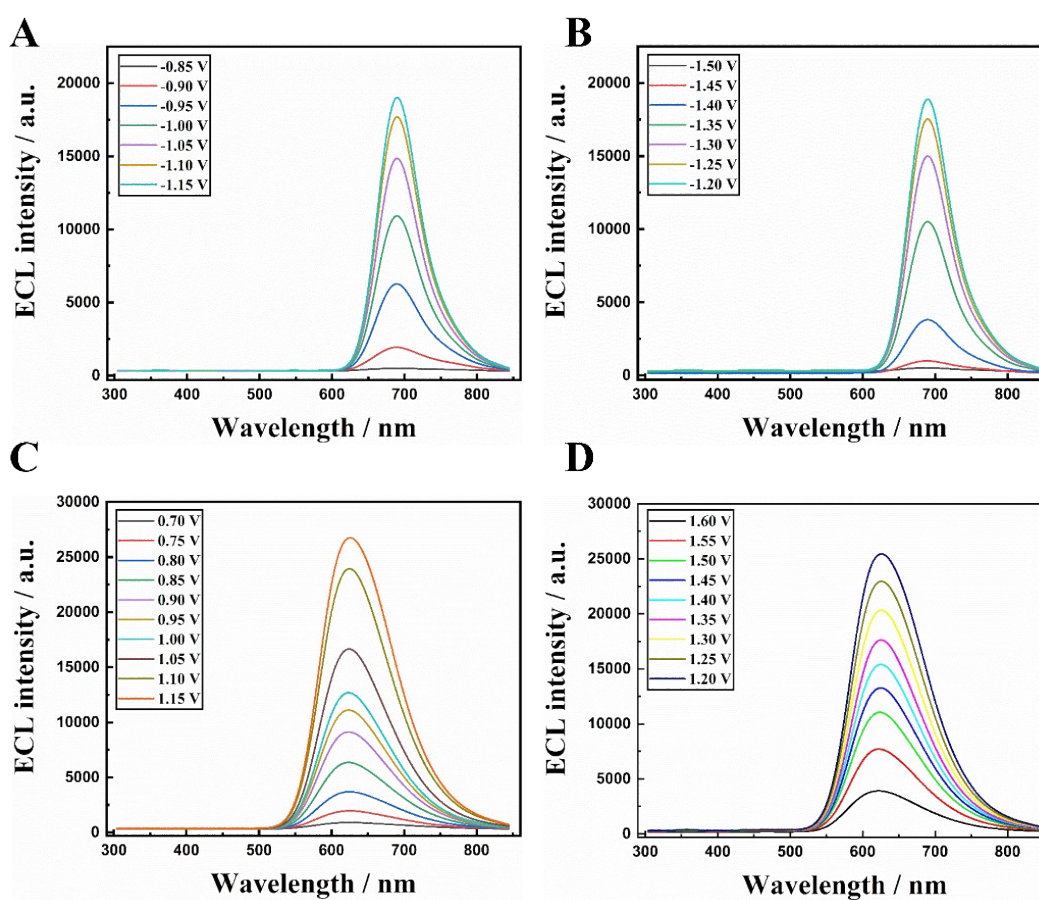


**Figure S5.** Spectra of ECL-1 (A and B) and ECL-2 (C and D) at different potentials. Reaction conditions: 0.01 M K<sub>2</sub>S<sub>2</sub>O<sub>8</sub> and 0.01 M TprA in 10 mM PBS buffer. Test conditions: sweep speed, 0.05 V/s.

### S7. Measurement of relative ECL efficiency

The relative ECL efficiency was calculated using the following equation with 1 mM Ru(bpy)<sub>3</sub><sup>2+</sup> as a reference<sup>2,3</sup>.

$$\Phi_{ECL} = \Phi_{ECL}^{\theta} \times \frac{I \times Q^{\theta}}{I^{\theta} \times Q} \quad (S1)$$

where  $I$  and  $I^{\theta}$  are the integrated ECL intensities (integrating ECL spectrum vs wavelength),  $Q$  and  $Q^{\theta}$  are the consumed charges (integrating current vs time),  $\Phi_{ECL}$  and  $\Phi_{ECL}^{\theta}$  are the ECL efficiency value of the sample and standard, respectively.

As a result, the relative ECL efficiency of ECL-1 was calculated to be 201.9 % relative to the  $\text{Ru}(\text{bpy})_3^{2+}/\text{K}_2\text{S}_2\text{O}_8$  standard and the relative ECL efficiency of ECL-1 was calculated to be 95.3 % relative to the  $\text{Ru}(\text{bpy})_3^{2+}/\text{TPrA}$  standard.

### S8. Influence of molar ratio of TCPP and $\text{Ru}(\text{bpy})_3^{2+}$ for ECL emissions

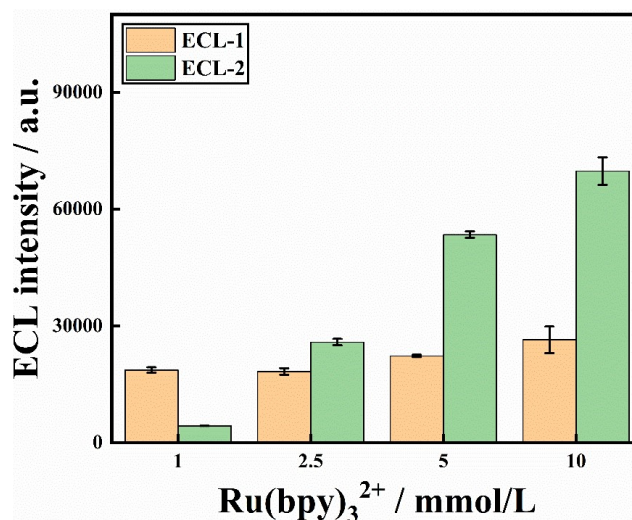


**Figure S6.** Influence of molar ratio of  $\text{Ru}(\text{bpy})_3^{2+}$  and TCPP in the process of synthesis for ECL emissions.

### S9. Effects of coreactant concentration on ECL

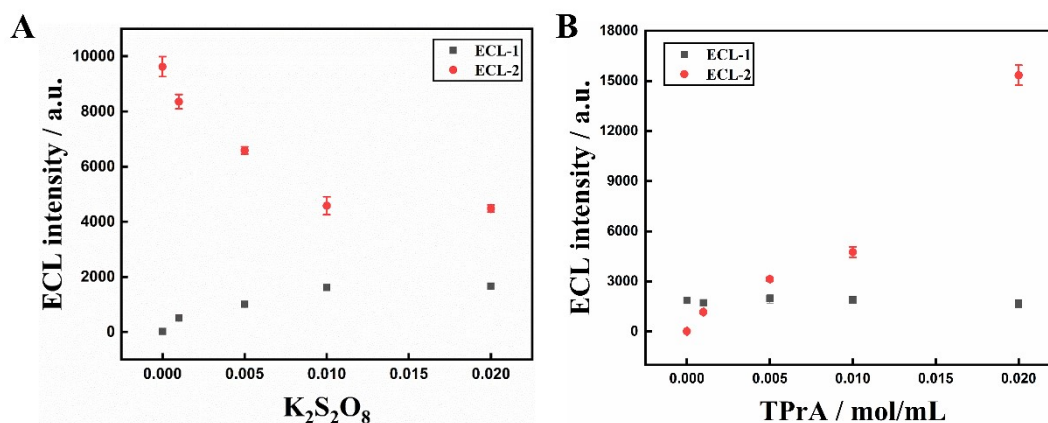


**Figure S7.** Effect of the concentration of coreactants on the intensities of ECL-1 and ECL-2: (A)  $K_2S_2O_8$  (TPrA, 0.01 mol/L) (B) TPrA ( $K_2S_2O_8$ , 0.01 mol/L).

**S10. Effects of various atmospheres on ECL**

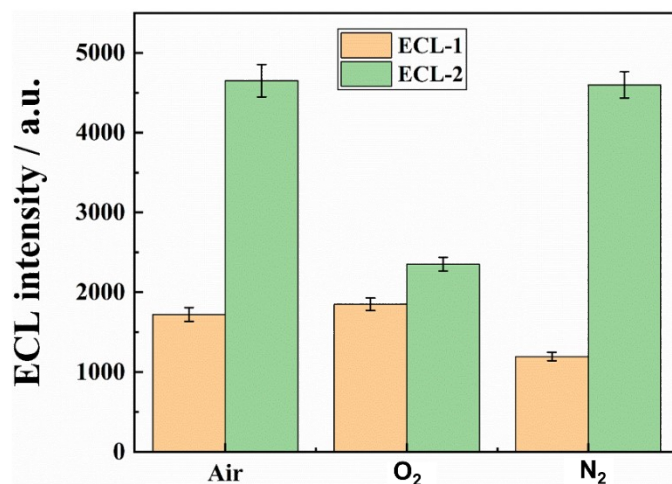


**Figure S8.** ECL intensities of TCPP@CRuSiO<sub>2</sub> nanoluminophores in O<sub>2</sub>, N<sub>2</sub> and air-saturated atmospheres. Test conditions: 0.01 M  $K_2S_2O_8$  and 0.01 M TPrA in 10 mM PBS buffer; scan rate: 0.05 V/s; PMT: -500 V.

## Reference

1. H. Ma, X. Li, T. Yan, Y. Li, H. Liu, Y. Zhang, D. Wu, B. Du and Q. Wei, *ACS applied materials & interfaces*, 2016, **8**, 10121-10127.
2. A. Kondyurin, K. Tsoutas, Q. X. Latour, M. J. Higgins, S. E. Moulton, D. R. McKenzie, and M. M. M Bilek, *ACS Biomater. Sci. Eng.* 2017, **3**, 2247-2258.
3. D. Luo, B. Huang, L. Wang, A. M. Idris, S. Wang, and X. Lu, *Electrochim. Acta.* 2015, 151, 42-49.